

World Journal of *Gastroenterology*

World J Gastroenterol 2020 August 21; 26(31): 4567-4728



REVIEW

- 4567 Current understanding of the metabolism of micronutrients in chronic alcoholic liver disease
Wu J, Meng QH

MINIREVIEWS

- 4579 COVID-19 pandemic: Pathophysiology and manifestations from the gastrointestinal tract
Galanopoulos M, Gkeros F, Doukatas A, Karianakis G, Pontas C, Tsoukalas N, Viazis N, Liatsos C, Mantzaris GJ

ORIGINAL ARTICLE**Basic Study**

- 4589 Feasibility and efficacy evaluation of metallic biliary stents eluting gemcitabine and cisplatin for extrahepatic cholangiocarcinoma
Xiao JB, Weng JY, Hu YY, Deng GL, Wan XJ

Case Control Study

- 4607 Establishment of a pattern recognition metabolomics model for the diagnosis of hepatocellular carcinoma
Zhou PC, Sun LQ, Shao L, Yi LZ, Li N, Fan XG

Retrospective Cohort Study

- 4624 Impact of interval between neoadjuvant chemoradiotherapy and surgery in rectal cancer patients
Mei SW, Liu Z, Wei FZ, Chen JN, Wang ZJ, Shen HY, Li J, Zhao FQ, Pei W, Wang Z, Wang XS, Liu Q

Retrospective Study

- 4639 Monocyte-to-lymphocyte ratio as a prognostic factor in peripheral whole blood samples of colorectal cancer patients
Jakubowska K, Koda M, Grudzińska M, Kańczuga-Koda L, Famulski W
- 4656 Clinical and prognostic significance of CC chemokine receptor type 8 protein expression in gastrointestinal stromal tumors
Li HL, Wang LH, Hu YL, Feng Y, Li XH, Liu YF, Li P, Mao QS, Xue WJ
- 4669 Initial experience of single-incision plus one port left-side approach totally laparoscopic distal gastrectomy with uncut Roux-en-Y reconstruction
Zhou W, Dong CZ, Zang YF, Xue Y, Zhou XG, Wang Y, Ding YL
- 4680 Prognostic value of pretreatment contrast-enhanced computed tomography in esophageal neuroendocrine carcinoma: A multi-center follow-up study
Zhou Y, Hou P, Zha KJ, Wang F, Zhou K, He W, Gao JB

- 4694 Clinical characteristics and risk factors for liver injury in COVID-19 patients in Wuhan

Zhang H, Liao YS, Gong J, Liu J, Zhang H

Observational Study

- 4703 Mucosal-associated invariant T cells in hepatitis B virus-related liver failure

Xue H, Li H, Ju LL, Han XD, Cheng TC, Luo X, Chen L, Shao JG, She YJ, Bian ZL

SYSTEMATIC REVIEWS

- 4718 Risk of malignancy in Caroli disease and syndrome: A systematic review

Fahrner R, Denmler SG, Inderbitzin D

ABOUT COVER

Editorial board member of *World Journal of Gastroenterology*, Dr. Tatsuo Kanda received an MD from the Niigata University School of Medicine (Japan) in 1991 and a PhD from the Graduate School of Medicine at Chiba University (Japan) in 1999. He then undertook post-doctoral training in the Departments of Pathology and Internal Medicine at Saint Louis University School of Medicine (United States) under the mentorship of Prof. Ratna B. Ray and Prof. Ranjit Ray, respectively. He returned to Japan and became an Associate Professor in the Department of Gastroenterology and Nephrology at Chiba University, Graduate School of Medicine in 2008. In his current roles as Associate Professor and Clinical Professor in the Division of Gastroenterology and Hepatology, Department of Medicine, Nihon University School of Medicine at Itabashi-ku, Tokyo, Japan, he performs clinical and basic research on hepatic and pancreatic diseases. (L-Editor: Filipodia)

AIMS AND SCOPE

The primary aim of *World Journal of Gastroenterology* (*WJG*, *World J Gastroenterol*) is to provide scholars and readers from various fields of gastroenterology and hepatology with a platform to publish high-quality basic and clinical research articles and communicate their research findings online. *WJG* mainly publishes articles reporting research results and findings obtained in the field of gastroenterology and hepatology and covering a wide range of topics including gastroenterology, hepatology, gastrointestinal endoscopy, gastrointestinal surgery, gastrointestinal oncology, and pediatric gastroenterology.

INDEXING/ABSTRACTING

The *WJG* is now indexed in Current Contents®/Clinical Medicine, Science Citation Index Expanded (also known as SciSearch®), Journal Citation Reports®, Index Medicus, MEDLINE, PubMed, PubMed Central, and Scopus. The 2020 edition of Journal Citation Report® cites the 2019 impact factor (IF) for *WJG* as 3.665; IF without journal self cites: 3.534; 5-year IF: 4.048; Ranking: 35 among 88 journals in gastroenterology and hepatology; and Quartile category: Q2.

RESPONSIBLE EDITORS FOR THIS ISSUE

Production Editor: *Yu-Jie Ma*; Production Department Director: *Xiang Li*; Editorial Office Director: *Ze-Mao Gong*.

NAME OF JOURNAL

World Journal of Gastroenterology

ISSN

ISSN 1007-9327 (print) ISSN 2219-2840 (online)

LAUNCH DATE

October 1, 1995

FREQUENCY

Weekly

EDITORS-IN-CHIEF

Andrzej S Tarnawski, Subrata Ghosh

EDITORIAL BOARD MEMBERS

<http://www.wjgnet.com/1007-9327/editorialboard.htm>

PUBLICATION DATE

August 21, 2020

COPYRIGHT

© 2020 Baishideng Publishing Group Inc

INSTRUCTIONS TO AUTHORS

<https://www.wjgnet.com/bpg/gerinfo/204>

GUIDELINES FOR ETHICS DOCUMENTS

<https://www.wjgnet.com/bpg/GerInfo/287>

GUIDELINES FOR NON-NATIVE SPEAKERS OF ENGLISH

<https://www.wjgnet.com/bpg/gerinfo/240>

PUBLICATION ETHICS

<https://www.wjgnet.com/bpg/GerInfo/288>

PUBLICATION MISCONDUCT

<https://www.wjgnet.com/bpg/gerinfo/208>

ARTICLE PROCESSING CHARGE

<https://www.wjgnet.com/bpg/gerinfo/242>

STEPS FOR SUBMITTING MANUSCRIPTS

<https://www.wjgnet.com/bpg/GerInfo/239>

ONLINE SUBMISSION

<https://www.f6publishing.com>

Basic Study

Feasibility and efficacy evaluation of metallic biliary stents eluting gemcitabine and cisplatin for extrahepatic cholangiocarcinoma

Jing-Bo Xiao, Jun-Yong Weng, Yang-Yang Hu, Gui-Long Deng, Xin-Jian Wan

ORCID number: Jing-Bo Xiao 0000-0002-3771-3034; Jun-Yong Weng 0000-0001-7803-2756; Yang-Yang Hu 0000-0002-1110-0678; Gui-Long Deng 0000-0002-2039-8779; Xin-Jian Wan 0000-0002-1202-7839.

Author contributions: Wan XJ conceived the study; Xiao JB mainly carried out the experiments and wrote the manuscript; Weng JY, Hu YY assisted in performing experiments; Deng GL performed the surgical procedures; Wan XJ supervised the study and revised the article.

Supported by the National Natural Science Foundation of China, No. 81870452 and No. 81470904; Science and Technology Development Funds of Shanghai of China, No. 16411952400.

Institutional review board statement: This study was approved by the Ethics Committee of Shanghai General Hospital, Shanghai Jiaotong University School of Medicine.

Institutional animal care and use committee statement: All experimental procedures were approved by the Animal Care and Use Committee of Shanghai General Hospital, Shanghai Jiaotong University School of Medicine.

Jing-Bo Xiao, Yang-Yang Hu, Xin-Jian Wan, Department of Gastroenterology and Shanghai Key Laboratory of Pancreatic Diseases, Shanghai General Hospital, Shanghai Jiaotong University School of Medicine, Shanghai 201620, China

Jing-Bo Xiao, Hospitalist and Internal Medicine Inpatient Department, Shanghai Jiahui International Hospital, Shanghai 200233, China

Jun-Yong Weng, Gui-Long Deng, Department of General Surgery, Shanghai General Hospital, Shanghai Jiaotong University School of Medicine, Shanghai 201620, China

Xin-Jian Wan, Department of Gastroenterology, Shanghai Jiao Tong University Affiliated Sixth People's Hospital, Shanghai 200233, China

Corresponding author: Xin-Jian Wan, MD, Chief Doctor, Department of Gastroenterology and Shanghai Key Laboratory of Pancreatic Diseases, Shanghai General Hospital, Shanghai Jiaotong University School of Medicine, No. 650 Xinsongjiang Road, Shanghai 201620, China. xinjian_wan_shsl@163.com

Abstract

BACKGROUND

Effective endoscopic management is fundamental for the treatment of extrahepatic cholangiocarcinoma (ECC). However, current biliary stents that are widely used in clinical practice showed no antitumor effect. Drug-eluting stents (DESs) may achieve a combination of local chemotherapy and biliary drainage to prolong stent patency and improve prognosis.

AIM

To develop novel DESs coated with gemcitabine (GEM) and cisplatin (CIS)-coloaded nanofilms that can maintain the continuous and long-term release of antitumor agents in the bile duct to inhibit tumor growth and reduce systemic toxicity.

METHODS

Stents coated with different drug-eluting components were prepared by the mixed electrospinning method, with poly-L-lactide-caprolactone (PLCL) as the drug-loaded nanofiber membrane and GEM and/or CIS as the antitumor agents. Four different DESs were manufactured with four drug-loading ratios (5%, 10%, 15%, and 20%), including bare-loaded (PLCL-0), single-drug-loaded (PLCL-GEM

Conflict-of-interest statement: All authors declare no conflicts of interest related to this article.

Data sharing statement: No additional data are available.

ARRIVE guidelines statement: The authors have read the ARRIVE guidelines, and the manuscript was prepared and revised according to the ARRIVE guidelines.

Open-Access: This article is an open-access article that was selected by an in-house editor and fully peer-reviewed by external reviewers. It is distributed in accordance with the Creative Commons Attribution NonCommercial (CC BY-NC 4.0) license, which permits others to distribute, remix, adapt, build upon this work non-commercially, and license their derivative works on different terms, provided the original work is properly cited and the use is non-commercial. See: <http://creativecommons.org/licenses/by-nc/4.0/>

Manuscript source: Unsolicited manuscript

Received: June 3, 2020

Peer-review started: June 3, 2020

First decision: June 18, 2020

Revised: June 30, 2020

Accepted: July 30, 2020

Article in press: July 30, 2020

Published online: August 21, 2020

P-Reviewer: de Moura EGH, Köksal AS

S-Editor: Zhang L

L-Editor: MedE-Ma JY

P-Editor: Ma YJ



and PLCL-CIS), and dual-drug-loaded (PLCL-GC) stents. The drug release property, antitumor activity, and biocompatibility were evaluated *in vitro* and *in vivo* to confirm the feasibility and efficacy of this novel DES for ECC.

RESULTS

The *in vitro* drug release study showed the stable, continuous release of both GEM and CIS, which was sustained for over 30 d without an obvious initial burst, and a higher drug-loaded content induced a lower release rate. The drug-loading ratio of 10% was used for further experiments due to its ideal inhibitory efficiency and relatively low toxicity. All drug-loaded nanofilms effectively inhibited the growth of EGI-1 cells *in vitro* and the tumor xenografts of nude mice *in vivo*; in addition, the dual-loaded nanofilm (PLCL-GC) had a significantly better effect than the single-drug-loaded nanofilms ($P < 0.05$). No significant differences in the serological analysis ($P > 0.05$) or histopathological changes were observed between the single-loaded and drug-loaded nanofilms after stent placement in the normal porcine biliary tract.

CONCLUSION

This novel PLCL-GEM and CIS-eluting stent maintains continuous, stable drug release locally and inhibits tumor growth effectively *in vitro* and *in vivo*. It can also be used safely in normal porcine bile ducts. We anticipate that it might be considered an alternative strategy for the palliative therapy of ECC patients.

Key words: Extrahepatic cholangiocarcinoma; Drug-eluting stent; Local chemotherapy; Gemcitabine; Cisplatin; Biliary obstruction

©The Author(s) 2020. Published by Baishideng Publishing Group Inc. All rights reserved.

Core tip: Drug-eluting stent is a new therapeutic concept for malignant biliary obstructions; however, studies on such stents have been limited, and all of them used single-drug-loaded nanofilms with a simple design and lacked complete serial *in vitro* and *in vivo* data. Our study was the first to apply dual chemotherapeutic medications to a drug-eluting stent with several improvements in the design compared to previous stents for the palliative therapy of extrahepatic cholangiocarcinoma, with a relatively complete preclinical evaluation. Our results indicate that this brand new stent can be a promising alternative to realize the dual functions of biliary drainage and local chemotherapy.

Citation: Xiao JB, Weng JY, Hu YY, Deng GL, Wan XJ. Feasibility and efficacy evaluation of metallic biliary stents eluting gemcitabine and cisplatin for extrahepatic cholangiocarcinoma.

World J Gastroenterol 2020; 26(31): 4589-4606

URL: <https://www.wjgnet.com/1007-9327/full/v26/i31/4589.htm>

DOI: <https://dx.doi.org/10.3748/wjg.v26.i31.4589>

INTRODUCTION

Cholangiocarcinoma (CCA) accounts for 7%-10% of all primary hepatobiliary malignancies worldwide^[1] and has an extremely poor prognosis. CCA is generally categorized as intrahepatic or extrahepatic (ECC) based on the anatomic location, and ECC patients usually present with signs and symptoms of biliary obstruction such as jaundice and acholic stool^[2]. Most patients present with advanced disease that is not amenable to surgery, due to a lack of sensitive, specific tumor markers^[3]. Thus, intervention with palliative endoscopic biliary drainage is essential to relieve jaundice and prevent cholangitis and hepatic failure and has been shown to improve quality of life^[4]. Clinically, biliary stents are widely used as palliative therapy for advanced ECC^[5], but the current stents provide only limited effect of biliary drainage and no antitumor activity. Even metal stents may become occluded over time due to tumor overgrowth or ingrowth, tissue hyperplasia, and biliary sludge^[6,7], which may result in progressive biliary obstruction and hepatic failure. The local application of chemotherapy drugs can maximize the drug concentration in the tumor microenvironment and reduce adverse reactions associated with systemic exposure

and nontarget organ toxicity^[8]. Therefore, drug-eluting stents (DESs) may be a promising approach for the treatment of ECC^[9].

To date, several kinds of biliary DESs have been designed and studied for the treatment of ECC. The first generation was paclitaxel-eluting covered metallic stents, and the data showed that they were probably safe but were not more advantageous than drug-free stents^[9-12]. Possible causes for these observations might include suboptimal stent design for the biliary anatomy and the weak effect of paclitaxel on ECCs^[13]. Other kinds of biliary DESs, such as gemcitabine-eluting, sorafenib-eluting, and vorinostat-eluting stents, have also been reported^[14-16]. These new DESs seem to be effective in inhibiting the proliferation of CCA cells; however, all of them are single-drug-loaded stents, and studies on the feasibility and safety of stent placement in the common bile duct (CBD) are lacking.

The current standard chemotherapeutic regimen for CCA is gemcitabine (GEM) plus cisplatin (CIS)^[17-19]. The combination of these two agents has shown improved survivability without substantial toxicity^[20,21]. Accordingly, we propose that local chemotherapy with two drugs is feasible and superior to a single drug. Therefore, we designed and fabricated novel GEM and CIS-eluting biliary stents using mixed electrospinning. In this study, we aimed to investigate the drug release property, antitumor activity, and biocompatibility *in vitro* and *in vivo* to evaluate the feasibility and efficacy of this novel stent for ECC.

MATERIALS AND METHODS

Fabrication of GEM and CIS-eluting biliary stents

Stents coated with GEM and CIS-eluting nanofiber membranes were fabricated by the mixed electrospinning method using an electrospinning machine (EBS ES-Biocoater; Nano NC, Seoul, South Korea) (Figure 1A). Poly- L-lactide-caprolactone (PLCL) was used as the drug carrier. The electrospinning solution (10% *w/v*) was prepared by dissolving 500 mg PLCL in 5 mL hexafluoroisopropanol. Then, different amounts of GEM/CIS (mass ratio 1:1) were added to this solution, and the final drug concentration was adjusted to 0%-20% (*w/w*) versus PLCL. The nickel-titanium metallic biliary stent (Micro-Tech Co., Ltd., Nanjing, China) covered with a PTFE inner coating membrane was 20 mm in length and 4 mm in diameter when fully expanded. The PTFE membrane was designed as an inner blocker to avoid drug loss of the bile flow and ensure maximum delivery into the tumor tissue. The stent was placed into a rolling collector (diameter 4 mm, length 15 cm, rolling speed 200 rpm, voltage 10 kV), and then 5 mL of the mixed electrospinning solution was transferred into a syringe with a 22G needle and sprayed onto the stent at a speed of 1.5 mL/h. Specifically, one PLCL-unloaded membrane was added to the drug-loaded stents as the outer layer to avoid drug burst release (Figure 1B). We prepared four types of DESs, namely, PLCL-0, PLCL-GEM, PLCL-CIS, and PLCL-GC (Figure 1C) (according to drug components), with different drug-loading ratios (0%, 5%, 10%, 15% and 20% (*w/w*)). Next, the drug-coated stent was carefully isolated from the collector and dried, weighed, and sterilized. For cell experiments and animal studies, different kinds of drug-incorporated nanofiber membranes were carefully separated from the stent and stored.

Characterization of the nanofiber films

The nanofiber morphology of the samples was observed under a scanning electron microscope (S-4800, Hitachi S-4800, Japan). In addition, to examine the ingredients of the nanofiber, Fourier transform infrared (FTIR) spectra were obtained by the potassium bromide disk method with an Avatar 380 FTIR instrument (Nicolet 6700, Thermo Fisher, United States).

In vitro drug release studies

The stents loaded with different drug components and loading ratios were placed into 15 mL centrifuge tubes separately ($n = 6$ in each group) with 10 mL phosphate-buffered saline (PBS, pH 7.4). Then, the tube was placed in a shaking incubator (HNYC-100D, Zhejiang NADE Scientific Instrument Co., China) at 100 rpm at 37 °C. At specific time intervals (1 d, 2 d, 3 d, 4 d, 5 d, 8 d, 11 d, 14 d, 19 d, 24 d, and 30 d), 1 mL of the media in the tube was taken to measure the released drug by high-performance liquid chromatography, and then an equal volume of fresh PBS was supplemented in each tube for continuous incubation. The cumulative drug release percentage was calculated as the actual cumulative drug release/total drug-loading capacity $\times 100\%$.

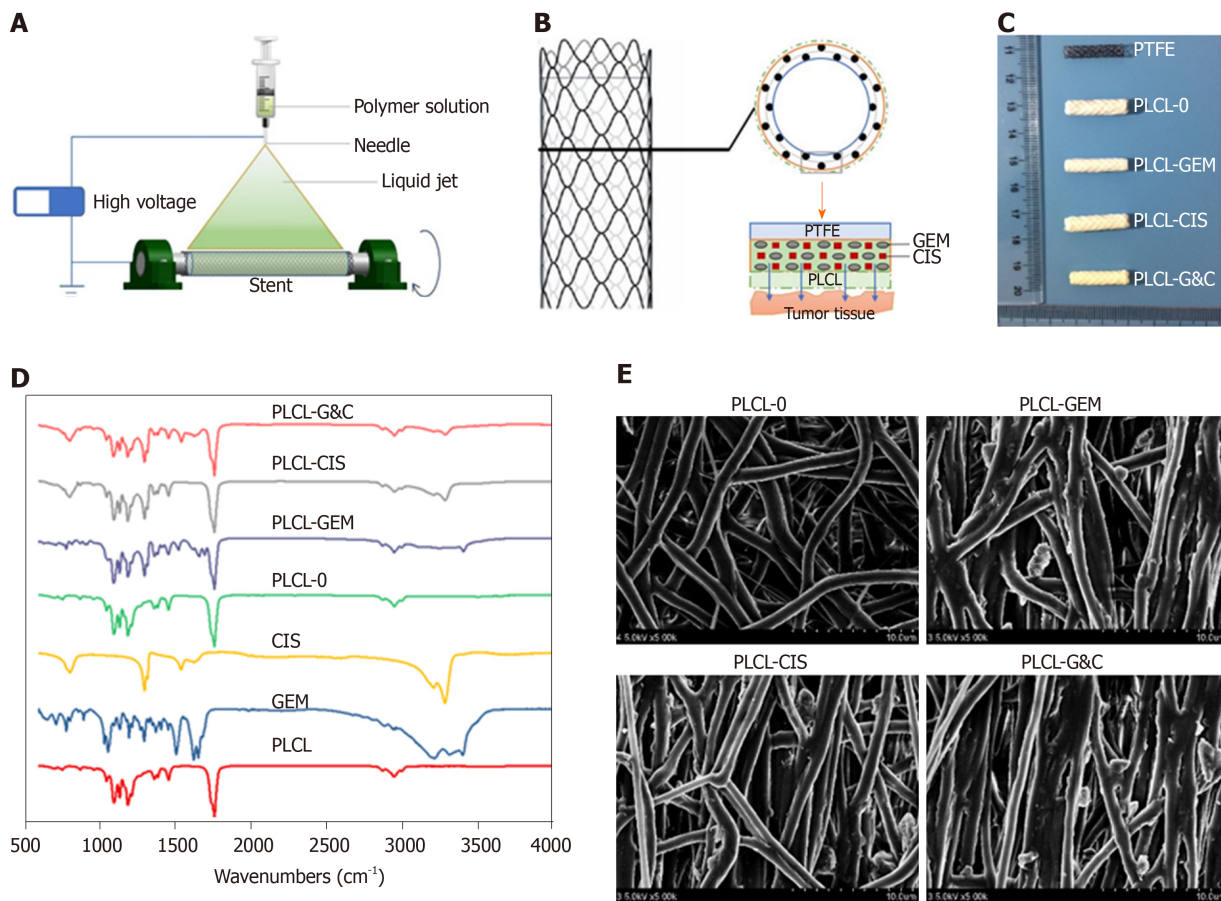


Figure 1 Manufacturing and characteristics of different biliary drug-eluting stents. A: Schematic illustration of the manufacturing of drug-eluting stents by the mixed electrospinning method; B: Optimized design of the gemcitabine/cisplatin-eluting biliary stent. The entire structure of the coated membranes consists of three layers: the inner polytetrafluoroethylene membrane (as a blocker to avoid drug loss), the middle PLCL layer (as the major drug carrier), and the outer PLCL-unloaded membrane (as a blocker to prevent burst release); C: Image of different types of drug-eluting stents; D: Fourier transform infrared spectra of different prototype drugs and drug-eluting nanofilms; E: Scanning electron microscope images of different drug-eluting nanofilms (magnification $\times 2000$). CIS: Cisplatin; GEM: Gemcitabine; PLCL: Poly-L-lactide-caprolactone; PLCL-0: Non-drug-loaded PLCL nanofilm; PLCL-CIS: PLCL nanofilm loaded with CIS; PLCL-GEM: PLCL nanofilm loaded with GEM; PLCL-GC: PLCL nanofilm loaded with both GEM and CIS; PTFE: Polytetrafluoroethylene.

Cell culture

The EGI-1 ECC cell line was obtained from the DSMZ (German Collection of Microorganisms and Cell Cultures; Braunschweig, Germany) and maintained in Dulbecco's modification of Eagle's medium (DMEM) containing 10% fetal bovine serum (FBS) and 1% penicillin-streptomycin at 37 °C in a 5% CO₂ incubator.

Antitumor activity study in vitro

EGI-1 cells were seeded into 96-well plates at a density of 4000 cells per well overnight in an incubator with 5% CO₂ at 37 °C. Following incubation, the cells were treated with GEM (0, 0.312, 0.625, 1.25, 2.5, 5, 10, and 20 $\mu\text{g}/\text{mL}$) or CIS (0, 0.312, 0.625, 1.25, 2.5, 5, 10, and 20 $\mu\text{g}/\text{mL}$) or their combinations for 24 h. To evaluate the antitumor activity of released drugs from the nanofiber membrane, a stent sample was immersed in serum-free DMEM into a 15 mL tube and treated as described previously. Drug-released media were collected every 24 hours and added to 96-well plates for incubation with EGI-1 cells. Cell viability after treatment was determined using a Cell Counting Kit 8 assay (Yeasen, Shanghai, China).

Calcein-AM/propidium iodide double staining

EGI-1 cells were seeded into a 6-well plate at a density of 1×10^6 cells/well and incubated with different kinds of drug-released media for 24 h. Then, the cells were digested, isolated, and costained with calcein-AM for living cells and propidium iodide for dead cells. Images were taken on a Leica DMi8 fluorescence microscope.

Scratch wound-healing assay

A scratch wound-healing assay was conducted to evaluate cell migration. After EGI-1 cells grew to form a confluent monolayer in a 6-well plate, a scratch was created along the central line of the well with a micropipette tip. Suspended cells were removed with PBS flushing, and the remaining cells were incubated with different kinds of drug-released media. Cells were photographed on a light microscope at 48 h.

Cell migration assay

In vitro cell migration assays were performed using a transwell chamber (Corning, United States) precoated with Matrigel (BD Biosciences, United States). EGI-1 cells (2×10^4) cultured in serum-free DMEM were seeded into the upper chamber. The lower chamber was filled with GEM/CIS-released media supplemented with 10% FBS. Cells that migrated to the reverse side of the membrane two days later were fixed with 4% paraformaldehyde and stained with Giemsa. The number of cells in 5 randomly selected microscopic fields per membrane was counted in each group.

In vivo tumor xenograft experiment

BALB/c nude mice (16-20 g, 4 wk old, male) were obtained from the Experimental Animal Center, Shanghai Jiaotong University. Mice were housed under a 12 h/12 h light/dark cycle at 22 ± 1 °C and 50% humidity and were given a standard chow diet with free access to food and drinking water. One hundred microliters of EGI-1 cells (2×10^6 /mouse) were injected subcutaneously into the right flank of each BALB/c mouse. Tumor diameters were measured every two days. When the tumor diameter reached nearly 5 mm, the following drug-eluting PLCL nanofilms were surgically implanted under the tumor: (1) None (nonimplanted group); (2) Empty PLCL nanofilm; (3) GEM-loaded nanofilm; (4) CIS-loaded nanofilm; and (5) GEM and CIS-loaded nanofilm ($n = 6$ in each group). Body weight and tumor volume were measured every 2 d after implantation using the formula: Volume = $1/2 \times \text{length} \times \text{width}^2$.

Histopathological analysis of the tumors

All the mice were sacrificed 4 wk later, and the tumors were harvested separately for further experiments. The tumor tissues were fixed with 4% paraformaldehyde, embedded in paraffin, and sectioned for hematoxylin and eosin (HE) staining. Additionally, to investigate the possible mechanisms involved, tumor tissues from extra groups of experimental mice were harvested one week after the implantation of drug-loaded nanofilms and subjected to a terminal deoxynucleotidyl transferase-mediated dUTP nick end labeling (TUNEL) assay (Abcam, England). Immunohistochemical staining was carried out with a cleaved caspase 3 antibody (CST, United States) at a dilution of 1:500 and an anti-PUMA (p53 upregulated modulator of apoptosis) (Abcam) antibody at a dilution of 1:200. Staining was performed using a Fast Red Substrate Kit (Abcam).

Stent placement in the CBD

Twenty-seven healthy Bama minipigs with an average weight of 25.7 ± 3.4 kg (Provided by Shanghai Jiaotong University School of Agriculture and Biology, Shanghai, China) were acclimatized to the following laboratory conditions: 22 ± 1 °C, 12 h/12 h light/dark cycle, 50% humidity and free access to food and drinking water. Pigs were randomly divided into five groups: Group A was sham operated ($n = 3$), group B received stent PLCL-0 ($n = 6$), group C received stent PLCL-GEM ($n = 6$), group D received stent PLCL-CIS ($n = 6$), and group E received stent PLCL-G&C ($n = 6$).

All the animals were fasted for 48 h before stent placement. Anesthesia was induced with an injection of 3% pentobarbital sodium (1 mL/kg) into the auricular vein. The pigs were positioned in a supine position. After a median incision was made in the upper abdomen and the CBD was successfully separated, a small incision was made above the CBD, through which the stent was placed into the CBD. The stent was then fixed on the bile duct wall with a 5.0 suture to avoid stent migration. For percutaneous cholangiography, we inserted a flexible tube cut from a scalp needle into the CBD towards the hepatic duct through the previous incision. Five mL contrast agent was injected into the CBD through the percutaneous tube, and the position of the stent was evaluated. The abdominal cavity was closed after cholangiography.

Hematologic examination

Serum samples were collected on day 0 (preoperation), 1, 3, 7, 14 and 28, and the serum white blood cell (WBC) count and alanine aminotransferase (ALT), aspartate

aminotransferase (AST), total bilirubin (TBil), γ -glutamyl transpeptidase (γ -GT), amylase and creatinine levels were measured to evaluate hepatorenal function and the inflammatory reaction after stent placement in all pigs.

Histologic analysis

All the animals were euthanized 4 wk after stent placement, and tissue samples, including the bile duct, liver, kidney, and duodenum, were harvested for histologic examination. The bile duct was removed from the hepatic bifurcation to the duodenum, including a portion of the duodenum and ampulla. The bile duct was then opened longitudinally, and each stent was gently removed. General morphological changes in the ductal mucosa and stents were evaluated. All the tissues were fixed with 4% paraformaldehyde for 24 h, and then HE staining and Masson trichrome staining were carried out. The thickness of the epithelial layers and the degree of submucosal inflammatory cell infiltration were evaluated in consensus by two experienced pathologists.

All animal experiments were approved by the Ethics Committee of Shanghai General Hospital.

Statistical analysis

All data were analyzed using SPSS version 23.0 (SPSS Inc., Chicago, Illinois, United States). Data are presented as the mean \pm standard deviation. Student's *t* test was used to compare continuous quantitative data between two groups, while differences between multiple groups were detected by analysis of variance. A two-tailed Wilcoxon signed-rank test was applied for ranked data. A *P* value < 0.05 was considered statistically significant.

RESULTS

Characteristics of GEM and CIS-eluting biliary stents

Four different GEM and CIS-loaded nanofilm-covered stents were manufactured by the mixed electrospray method (Figure 1C). As shown in the FTIR spectra (Figure 1D), extra peaks (seen at 3300 cm^{-1} to 3500 cm^{-1} and at 700 cm^{-1} to 1700 cm^{-1}) were observed in the PLCL-GEM, PLCL-CIS, and PLCL-G&C polymers loaded with drugs, while they were absent in the pure PLCL polymer. The fiber morphology characterized by scanning electron microscopy is shown in Figure 1E. Pure PLCL nanofibers were smooth, while drug-loaded polymers were scattered with drug particles of relatively equal sizes. All these results demonstrated successful drug loading into the nanofibers.

Drug release in vitro

GEM-loaded nanofibers with different drug-loading ratios exhibited similar release behaviors *in vitro*, while nanofibers with a low drug-loading ratio released relatively faster than those with a high drug-loading ratio (Figure 2A). The release of GEM consisted of three phases: The initial rapid release phase (day 0-10, cumulative release for 75% of the total drug-loading amount), the medium-term stable phase (day 11-20, steady and gentle release for 85%), and the late terminal platform phase (day 21-30, nearly complete release for $\geq 95\%$).

The release of CIS consisted of two phases: The initial phase (day 0-7, cumulative release for 15%-20%) and the uniform-stable phase (day 8-30, cumulative release for 25%-35%) (Figure 2B). The release of CIS was different from that of GEM. First, nanofibers with a drug-loading ratio of 5% released faster than those with other drug-loading ratios, while no significant difference was observed between nanofibers with high drug-loading ratios in the initial phase. Second, a significant gap in the release percentage was observed over time. Third, the total released amount of CIS at the end of the observation period was much lower than that of GEM.

This difference is mainly due to the different solubilities of GEM and CIS. The solubility of GEM is higher than that of CIS at 37 $^{\circ}\text{C}$, so it is easier for GEM to be released from PLCL nanofibers. In the first stage, the primary mechanism for drug release is dissolution so that drugs can be released rapidly, especially GEM. In the subsequent phase, a combination of diffusion and degradation become the major forms of drug release; due to the long distance for diffusion from the internal membrane and the relatively slow PLCL degradation rate, the drug release rate during this period gradually slows and can be maintained to a near-constant degree.

The release of GEM (Figure 2C-a) and CIS (Figure 2C-b) from PLCL-GEM and CIS-

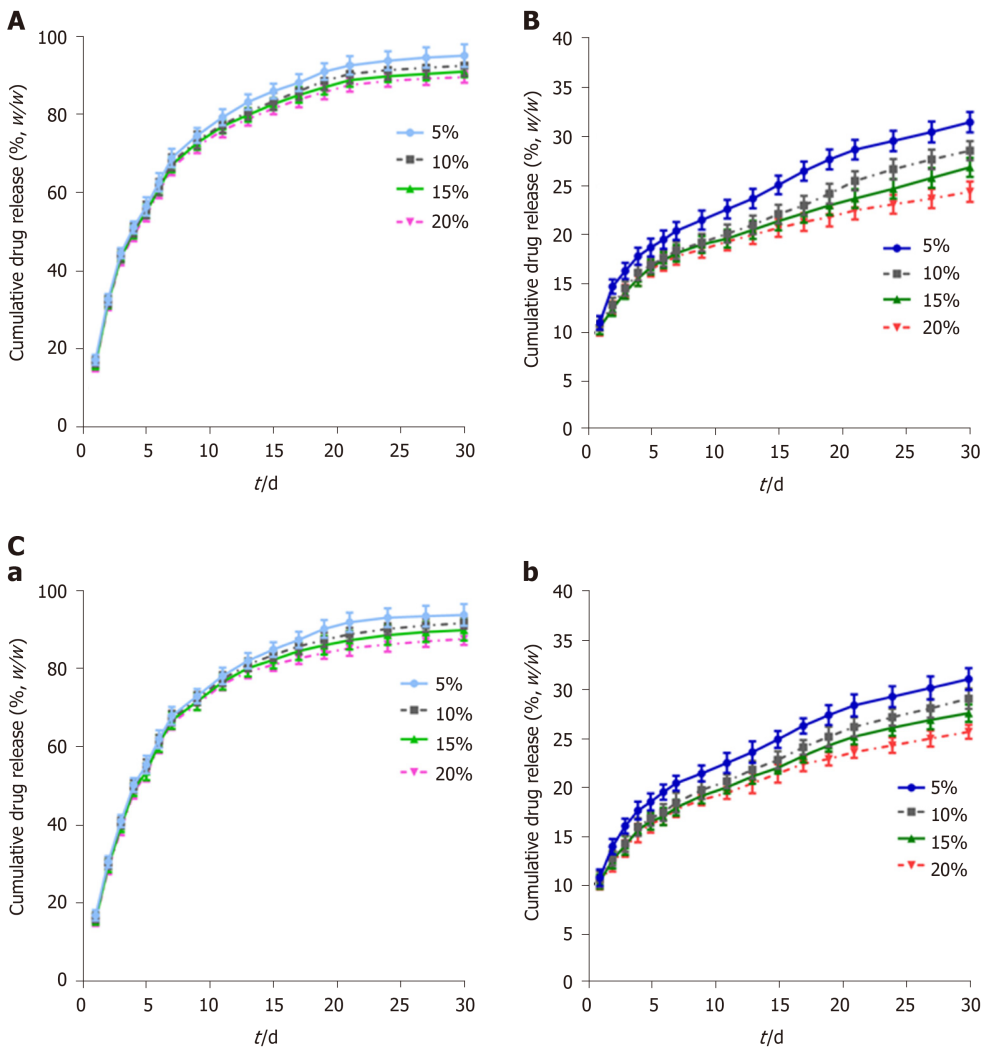


Figure 2 Cumulative drug release of different biliary drug-eluting stents with different drug-loading ratios. A: Release curves of gemcitabine from PLCL-GEM-eluting stents; B: Release curves of cisplatin from PLCL-CIS-eluting stents; C: Release curves of (a) gemcitabine and (b) cisplatin from PLCL-GEM and CIS-eluting stents. CIS: Cisplatin; GEM: Gemcitabine; PLCL: Poly-L-lactide-caprolactone.

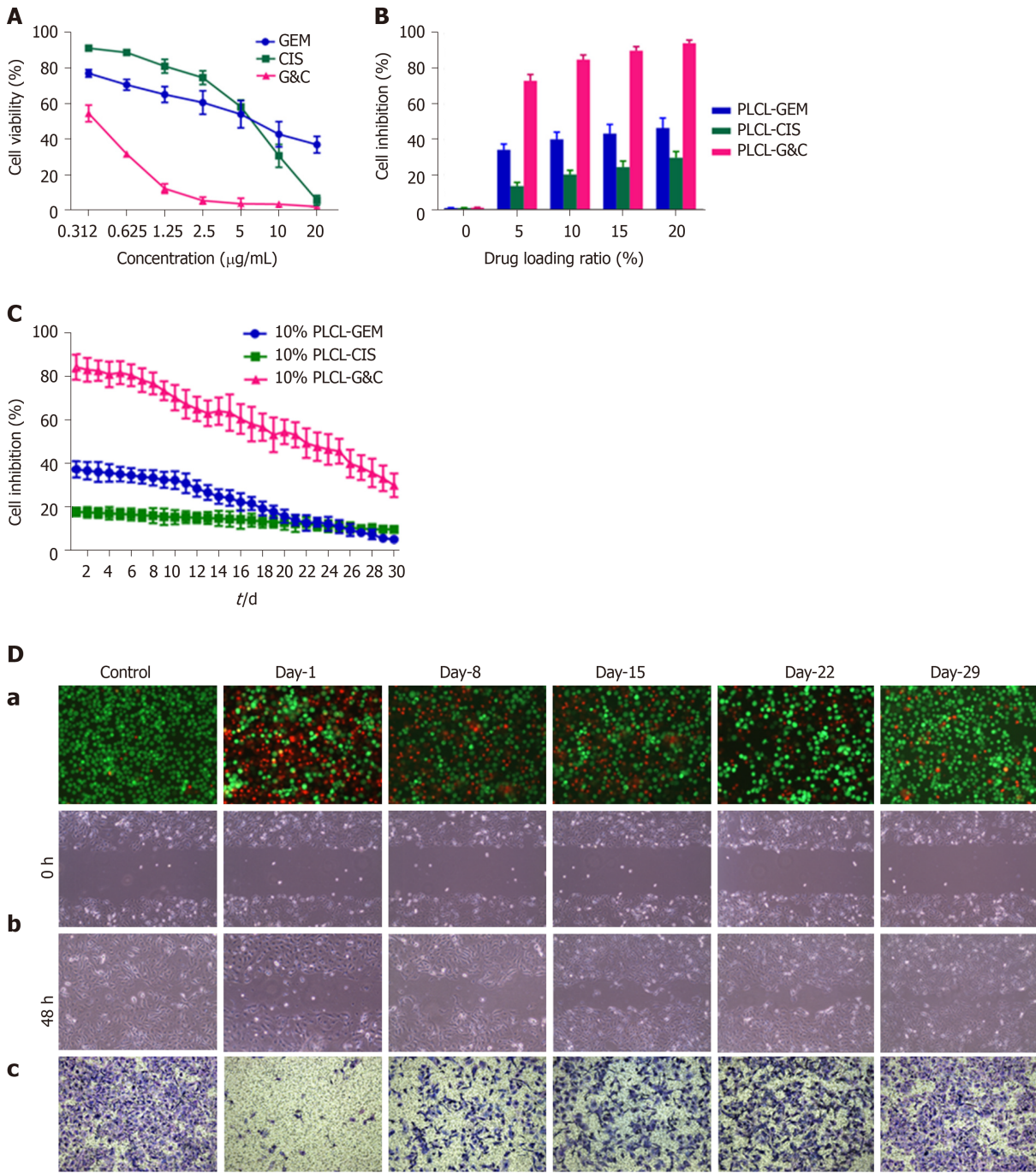
coloaded nanofibers was similar to the single-drug-loaded nanofibers, albeit with a slightly slower release rate.

Antitumor activity of PLCL-GEM and CIS nanofilms against EGI-1 cells *in vitro*

The antitumor activity of GEM and CIS-loaded nanofilms was assessed by examining the viability, migration, and invasion of EGI-1 cholangiocarcinoma cells *in vitro*, as shown in Figure 3.

The viability of EGI-1 cells decreased following incubation with GEM or CIS in a dose-dependent manner, and the half-maximal inhibitory concentration (IC_{50}) was 4.625 $\mu\text{g}/\text{mL}$ for GEM and 5.933 $\mu\text{g}/\text{mL}$ for CIS (Figure 3A). We initially set the drug-loading ratio at 1:1 due to the close IC_{50} of these two drugs. Then, we prepared 4 types of polymer films containing different drug compositions (PLCL-0, PLCL-GEM, PLCL-CIS, and PLCL-G&C) at 4 drug-loading ratios (5%, 10%, 15%, and 20%). The effect of drug-released media from the first 24 h in the polymer films on the proliferation of EGI-1 cells was tested (Figure 3B). The growth inhibition of EGI-1 cells increased in a loading ratio-dependent manner, and GEM and CIS-coated films caused significantly more growth inhibition than single-drug-loaded films ($P < 0.001$). To ensure inhibitory efficiency and reduce the side effects and drug dose, we set the initial inhibition rate of coloaded film to $> 80\%$ as a standard and assumed that a drug-loading ratio of 10% might be ideal for further experiments.

We continuously tested the antitumor effect of the drug release solution from polymer films loaded with 10% drugs on EGI-1 cells for 30 d (Figure 3C). During the observation period, the single-drug-loaded films had a certain inhibitory effect in the early stage, and the effects of PLCL-GEM were stronger than those of PLCL-CIS.



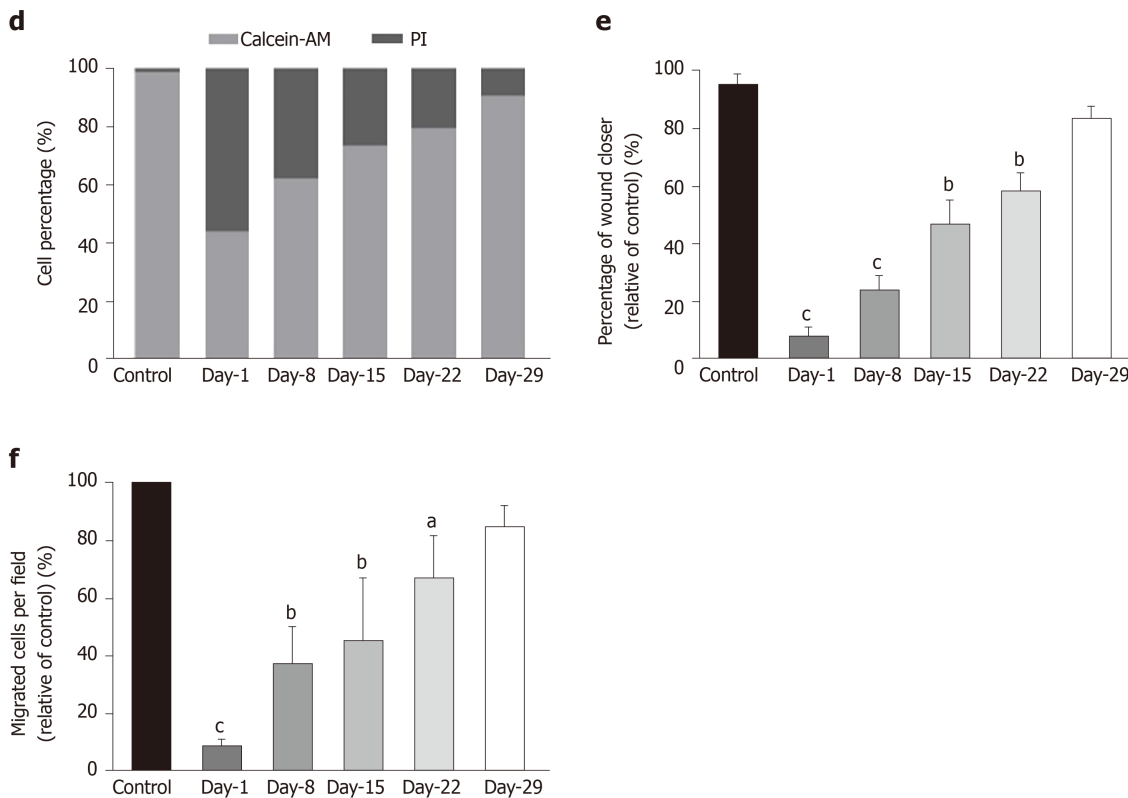


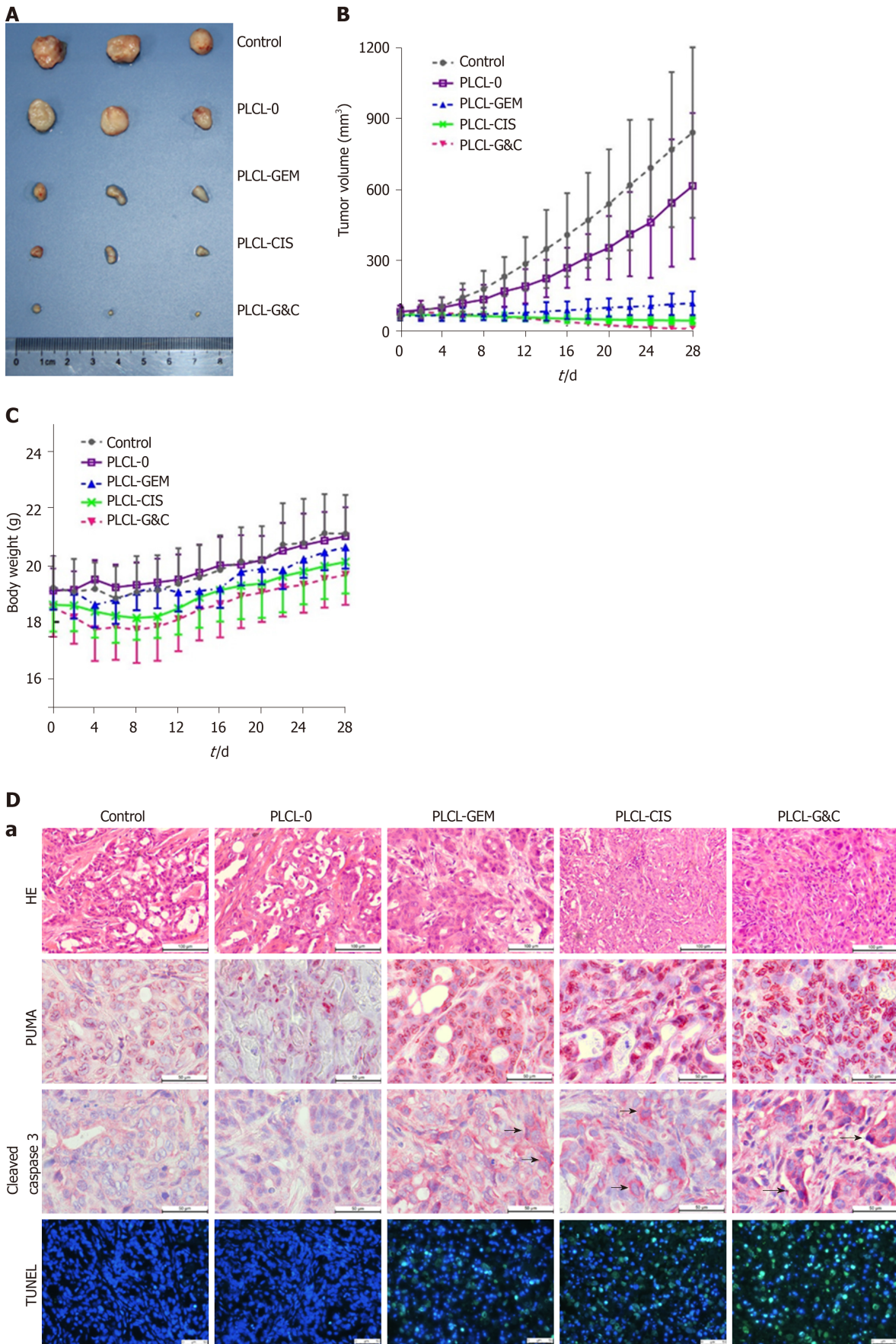
Figure 3 Antitumor activity of different drug-loaded nanofilms against human cholangiocarcinoma cells *in vitro*. A: Effects of different concentrations of prototype gemcitabine and cisplatin on the growth of EGI-1 cells; B: Inhibition of EGI-1 cells caused by different drug-loaded nanofilms with different drug-loading ratios for 30 d; C: Inhibition of EGI-1 cells caused by drug-released media from 10% drug-loaded nanofilms every other week for 30 d; D: Effects of 10% drug-loaded nanofilms on the (a) viability (magnification $\times 100$); (b) migration ($\times 100$); (c) and invasion ($\times 200$) of EGI-1 cells; (d) statistical analysis of the proportion of living and dead cells coincubated with different drug-released media; (e) quantitative analysis of the wound closer area following coincubation with different drug-released media; and (f) quantification of migrated cells coincubated with different drug-released media. ^a $P < 0.05$, ^b $P < 0.01$, ^c $P < 0.001$ vs control ($n = 6$ mice per group). CIS: Cisplatin; GEM: Gemcitabine; PI: Propidium iodide; PLCL: Poly-L-lactide-caprolactone; PLCL-CIS: PLCL nanofilm loaded with CIS; PLCL-GEM: PLCL nanofilm loaded with GEM; PLCL-GC: PLCL nanofilm loaded with both GEM and CIS.

However, over time, the effect of PLCL-GEM decreased beginning on day 10 and diminished significantly in the later period; the effect of PLCL-CIS was relatively weak, but it was maintained to some extent and decreased gradually without a significant fall peak in the middle and later stages. This was consistent with the release property of GEM and CIS from the polymer film. The PLCL-GC polymer film exhibited excellent inhibitory capability due to mutual compensation for dual drug release: It showed a stronger effect in the early stage than the single-drug-loaded polymer film that was maintained appropriately in the later stage. The inhibition rate was approximately 30% at the end of the observation period. Therefore, we believe that the continuous release and cumulative effect of the coloaded drugs ensure that this novel DES plays an ideal role in inhibiting tumor cell proliferation.

We then studied the effects of drug-released media from PLCL-10% GC on the viability, migration, and invasion of EGI-1 cells at specific time points (day 1, 8, 15, 22, and 29; every other week) (Figure 3D). The viability (Figure 3D-a), migration (Figure 3D-b), and invasion (Figure 3D-c) of EGI-1 cells were inhibited by incubation with the released GEM and CIS from the nanofilms during the 30-d drug release period. All the effects were relatively strong in the early phase and then decreased gradually but were still maintained in the later period. These results indicate that the viability inhibition, anti-migration, and anti-invasion capacities of the loaded GEM and CIS from this novel DES are maintained during the drug release period.

Antitumor activity of PLCL-GEM and CIS nanofilms in an animal tumor xenograft model

We used an animal tumor xenograft model to study the anticancer activity of the drug-loaded nanofilms *in vivo*. Tumor mass from nude mice after implantation of different nanofilms for 28 d is shown in Figure 4A. The tumor sizes in the drug-loaded groups were visually smaller than those in the unloaded and control groups. All drug-loaded



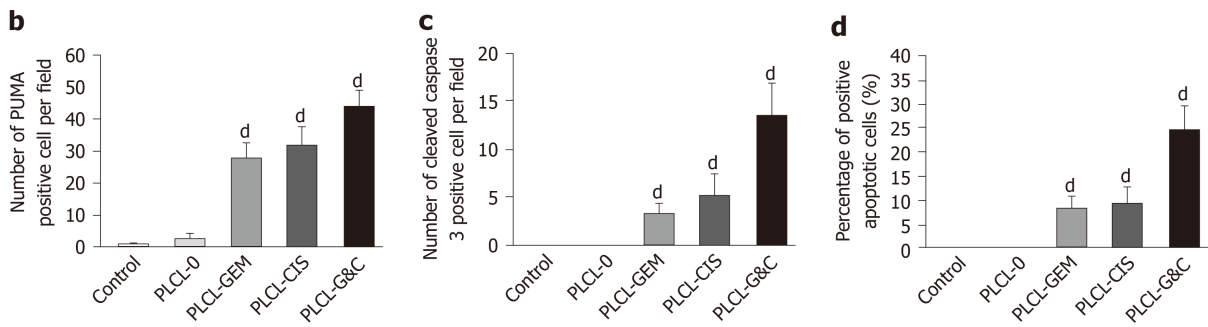


Figure 4 Antitumor activity of drug-loaded nanofilms against subcutaneous tumor xenografts in nude mice *in vivo*. A: Image of subcutaneous tumors from nude mice after drug-loaded nanofilm implantation for 4 wk; B: Changes in tumor volume; C: Changes in body weight; and D: (a) HE staining (magnification $\times 200$, scale bar $100\ \mu\text{m}$), immunohistochemical analysis of p53 upregulated modulator of apoptosis and cleaved caspase-3 ($\times 400$, scale bar $50\ \mu\text{m}$), and terminal deoxynucleotidyl transferase-mediated dUTP nick end labeling staining ($\times 200$, scale bar $50\ \mu\text{m}$) in subcutaneous tumor tissues; (b-d) Statistical analysis results: Quantification of (b) p53 upregulated modulator of apoptosis-positive cell numbers, (c) cleaved caspase-3-positive cell numbers, and terminal deoxynucleotidyl transferase-mediated dUTP nick end labeling-positive cell proportion in subcutaneous tumor tissues. $^{\text{d}}P < 0.001$ vs control ($n = 6$ mice per group). CIS: Cisplatin; GEM: Gemcitabine; HE: Hematoxylin and eosin; PLCL: Poly L-lactide-caprolactone; PLCL-0: Non-drug-loaded PLCL nanofilm; PLCL-CIS: PLCL nanofilm loaded with CIS; PLCL-GEM: PLCL nanofilm loaded with GEM; PLCL-GC: PLCL nanofilm loaded with both GEM and CIS; PUMA: p53 upregulated modulator of apoptosis; TUNEL: Terminal deoxynucleotidyl transferase-mediated dUTP nick end labeling.

films gradually inhibited tumor growth, while PLCL-GC exerted the most ideal suppression effect according to the tumor growth curve (Figure 4B). In addition, tumor growth was partially inhibited in the PLCL-unloaded film group compared to that in the sham-operated group. This observation was probably due to the suppression effect of the nanofilm on vascular reconstruction and contact growth inhibition, which made tumor proliferation relatively limited.

The weight change curves of the PLCL-unloaded group and the sham-operated group were similar, with no significant difference ($P > 0.05$). However, varying degrees of weight loss were observed in the drug-loaded groups during the initial period (Figure 4C). The PLCL-GEM nanofilm-implanted group experienced faster weight recovery than the other two groups, and weight recovery steadily increased, consistent with that observed in the control group. The PLCL-GC group seemed to lose the most body weight but still recovered and gained extra body weight at the end of the observation period.

The weight loss of experimental animals might be caused by the side effects of chemotherapeutics. Due to the relatively large ratio of the nanofilm area to the body surface and the numerous vascular networks on the backs of nude mice, drugs can be easily absorbed and transferred to the whole body, causing toxicity similar to that observed with systemic chemotherapy. Thus, the weight loss of dual-loaded nanofilms was more significant than that of single-drug-loaded nanofilms.

HE staining of tumor tissues showed reduced pathological karyokinesis and collagen fibroplasia in the drug-loaded groups (Figure 4D-a). The expression of apoptosis-related proteins, such as PUMA (Figure 4D-b) and cleaved caspase-3 (Figure 4D-c), and the number of TUNEL-positive cells (Figure 4D-d) in tumor tissues were all increased with the implantation of drug-loaded nanofilms, indicating that the suppression of tumor growth might be due to the activation of apoptosis-related molecular signals.

All these results suggest that the drug-loaded nanofilms efficiently exert their antitumor effects in mouse tumor xenografts *in vivo*, and the dual-loaded nanofilm was superior to the single-drug-loaded nanofilm.

Feasibility and safety in the porcine biliary tract

All stents were successfully placed in porcine biliary tracts without procedure-related complications. Cholangiography confirmed the stent position and patency in the CBD (Figure 5A-b). One case of incisional hernia occurred in the PLCL-0 stent group. No perforation, cholangitis, stent migration, or occlusion occurred in any group, and all porcine survived until euthanization for histopathological analysis 4 wk after stent placement.

Serum ALT, AST, γ -GT, and amylase levels were elevated, with mild to moderate abnormal levels (< 3 -5 upper limit of normal, ULN) during the first week after stent placement, mainly due to the surgical procedure and biliary stricture. All these parameters gradually returned to normal after 4 wk (Supplementary material Table 1,

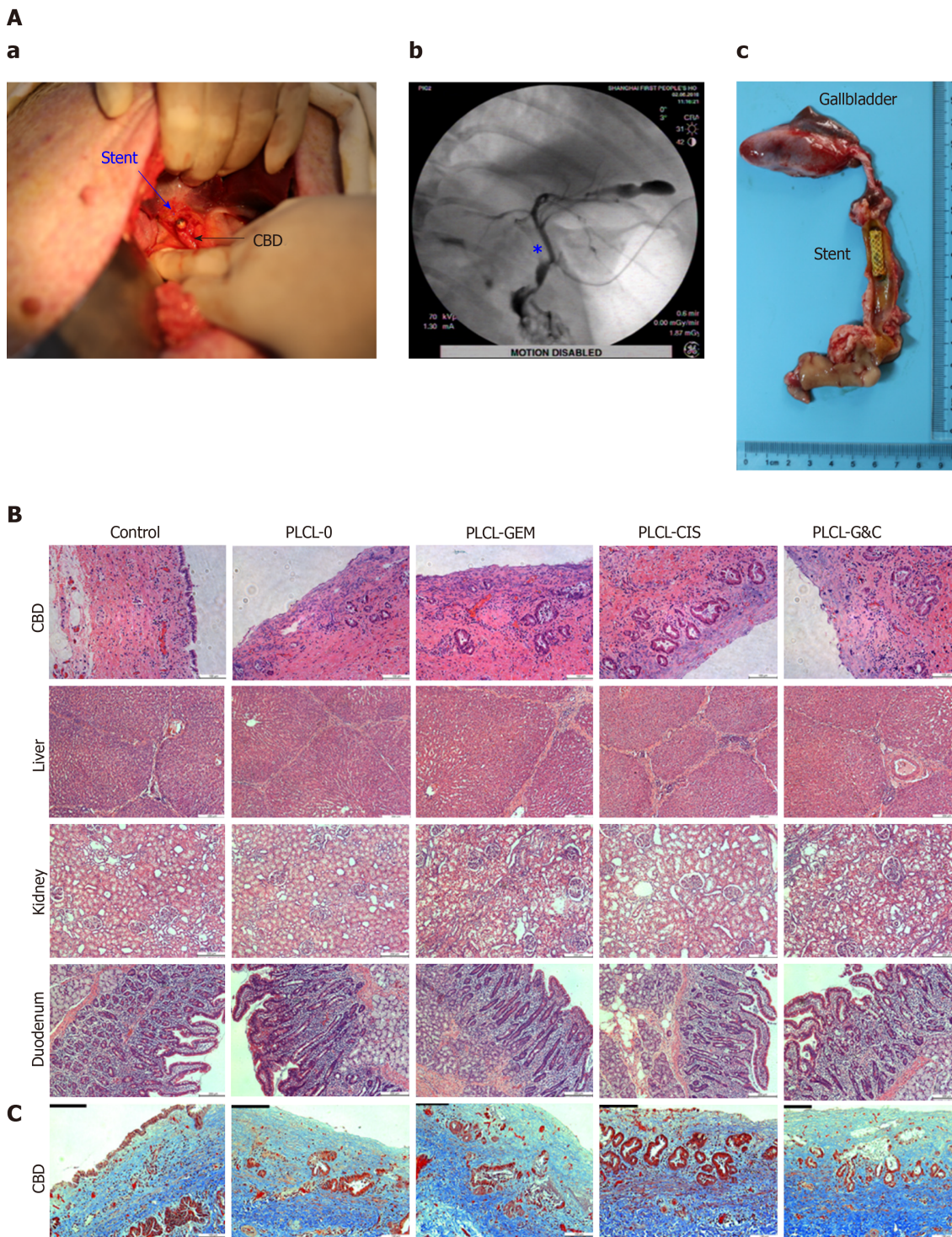


Figure 5 Safety evaluation of different drug-eluting biliary stents in a porcine model. A: (a) Critical surgical step necessary to place a stent into the porcine CBD; the stent was sutured on the CBD wall carefully when closing the CBD to avoid stent migration; (b) cholangiogram after stent placement; the pentacle marks the location of the stent; (c) macroscopic appearance of the CBD after animals were sacrificed; all the stents were still in the CBD and had not migrated; B: HE staining of the CBD (magnification $\times 200$, scale bar $100\ \mu\text{m}$), liver, kidney, and duodenum ($\times 100$, scale bar $200\ \mu\text{m}$) 30 d after placement of different drug-eluting biliary stents; C: Masson trichrome staining of the CBD 30 d after placement of different drug-eluting biliary stents ($\times 200$, scale bar $100\ \mu\text{m}$). CBD: Common bile duct; CIS: Cisplatin; GEM: Gemcitabine; PLCL: Poly-L-lactide-caprolactone; PLCL-0: Non-drug-loaded PLCL nanofilm; PLCL-CIS: PLCL nanofilm loaded with CIS; PLCL-GEM: PLCL nanofilm loaded with GEM; PLCL-GC: PLCL nanofilm loaded with both GEM and CIS.

available online), and no differences were observed between groups ($P > 0.05$ for all).

The gross appearance of the bile duct mucosa from the 5 groups was similar, and no ulceration, perforation, or necrosis was observed (Figure 5A-c). In addition, no apparent luminal dilation, wall thinning, or mucosal hyperplasia was observed along the bile duct segment that had been stented.

Microscopically, epithelial layer thickness was more obvious in the stent-implanted

groups than in the sham-operated group, with a multilayered epithelium instead of a normal single layer of cuboidal epithelium, which might be a chronic adaptive change to the compression and dilation of the stent. However, no significant difference was observed between the stented groups (Figure 5B, Table 1). The CBD wall of the stented segments presented mild inflammation in the non-drug-loaded group, and drug-loaded components seemed to increase the degree of inflammatory cell infiltration. In addition, cisplatin in the membrane was associated with inflammatory reactions in the mucosa and submucosa (Figure 5B, Table 1). Masson trichrome staining revealed a similar extent of fibrotic reactions without fibromuscular wall thickening or collagen fiber homogenization in the submucosal layer of stented segments in all groups, suggesting that fibrotic reactions are not dependent on drug-loaded components (Figure 5C). No granulation, atrophy or necrosis was observed in any group. In addition, no histological changes in the duodenum, liver, or kidney were observed in any group (Figure 5B).

In conclusion, *in vivo* experiments confirmed that the DES has good safety and biocompatibility in the normal porcine biliary tract.

DISCUSSION

Currently, ECC is rarely curable and is associated with a poor prognosis. The therapeutic resistance of ECC is mainly due to its highly desmoplastic nature, rich tumor microenvironment, and profound genetic heterogeneity^[2]. Although a few breakthroughs and progress in the treatment of ECC have been made since comprehensive cancer therapies, such as targeted therapy and immunotherapy, the mortality has not been significantly decreased. According to the newest NCCN guidelines, the primary therapeutic strategy for unresectable ECC is still biliary drainage, if indicated GEM/CIS combination therapy is also used^[23]. However, endoscopic stent placement for the palliation of malignant biliary obstruction is associated with a high failure rate since reocclusion is common after stent implantation^[5,8]. In addition, patients under systemic chemotherapy with GEM/CIS tend to suffer from toxic side effects such as myelosuppression, digestive tract reactions, hepatotoxicity, and nephrotoxicity^[17-19]. Therefore, a new concept of a "therapeutic stent" was proposed to achieve local antitumor therapy for ECC. First, local chemotherapy may maximize the drug concentration in the tumor microenvironment and reduce toxicity on nontarget organs through systemic distribution^[8]. It may also reduce the required drug dose and thus save costs. Second, the local inhibition of tumor proliferation may prevent stent stenosis or obstruction from tumor ingrowth or epithelial overgrowth in an advanced stage^[7]. This may result in a prolonged patency time and biliary drainage to reduce the risk of cholangitis, progressive jaundice, or even biliary sepsis. We propose that this therapeutic stent will help improve the survival and quality of life of ECC patients.

DES is a promising therapy, and its effective design realizes the dual function of biliary drainage and local chemotherapy in malignant biliary obstructions. Relevant studies have been published, including those on esophageal cancer^[24,25], colorectal cancer^[26,27], and bile duct cancer^[6,9-12,15,28-30]. Most of the biliary stents used in earlier studies were paclitaxel-eluted stents, and there seemed to be no improvement in the duration of stent patency or survival time compared to unloaded stents in several prospective pilot studies^[10,12]. Possible reasons for these findings may be nonoptimal medications and poor drug release to maintain sufficient local antitumor activity. However, these studies still demonstrated the safety and feasibility of the application of DESs in patients with ECC. DESs loaded with other antitumor agents, including gemcitabine^[29], sorafenib^[15], and vorinostat^[30], have also been investigated for safety and efficacy in malignant biliary obstruction. These DESs were all single-drug-loaded stents with a simple design and lacked complete serial *in vitro* and *in vivo* data. Our study was the first to apply dual chemotherapeutic medications to DESs for the management of ECC with a relatively complete preclinical evaluation.

The debate concerning the choice between fully covered self-expanding biliary metal stents (FCSEMSs) and uncovered self-expandable metal stents in patients with malignant biliary stricture has been protracted in the medical literature and is still ongoing^[31]. Some researchers demonstrated that covered stents were associated with increased rates of migration and cholecystitis^[32,33], while others reported no statistically significant difference between them^[34-36]. Since no official guideline or conclusive evidence has been established so far, the stent type should be selected on an individualized basis. Notably, inflammatory cell infiltration and mucosal hyperplasia

Table 1 Epithelial layer thickness and inflammation in the common bile duct after stent placement

	Thickness of the epithelial layer (μm)	Degree of inflammatory cell infiltration			
		-	+	++	+++
Control ($n = 3$)	103 \pm 24.1	1	2	0	0
PLCL-0 stent ($n = 6$)	209 \pm 45.4 ^a	0	5	1	0
PLCL-GEM stent ($n=6$)	259 \pm 77.3 ^a	0	4	2	0
PLCL-CIS stent ($n=6$)	255 \pm 64.2 ^a	0	3	3	0
PLCL-GC stent ($n=6$)	287 \pm 81.8 ^a	0	3	3	0
<i>P</i> value		0.157			

None (-), mild (+), moderate (++), and severe (+++).

^a $P < 0.05$ vs control. CBD: Common bile duct; CIS: Cisplatin; GEM: Gemcitabine; PLCL: Poly- L-lactide-caprolactone; PLCL-0: Non-drug-loaded PLCL nanofilm; PLCL-CIS: PLCL nanofilm loaded with CIS; PLCL-GEM: PLCL nanofilm loaded with GEM; PLCL-GC: PLCL nanofilm loaded with both GEM and CIS.

were reported to be more obvious in uncovered stents than in covered stents^[37]. In DESs with a partially covered design (due to concerns associated with stent migration), these histological changes were severe in the biliary mucosa in contact with the bare ends of the stent^[9]. Of note, Wang and colleagues developed partially covered nitinol stents loaded with 5-fluorouracil or paclitaxel for esophageal cancer and found severe tissue responses, including inflammation, ulceration, and granulation, at the bare ends compared to the drug-loaded part in porcine esophageal tissues^[25]. Since partially covered stents have not yet been proven to be effective in the prevention of stent migration for malignant biliary strictures and still need to be further evaluated in clinical trials^[38,39], in our study, we used a fully covered stent design to alleviate tissue responses.

We also made several improvements in the design of our DES based on the experience of the initial paclitaxel-eluted stents in the early stage. First, we chose the first-line chemotherapeutic medications GEM plus CIS as the loaded drugs on the assumption that dual drugs would be superior to single drugs in local antitumor activity. Second, we used the PTFE membrane as the inner blocker to (1) ensure unidirectional drug release to the tumor tissue side to avoid fluctuation release and drug loss by bile flow; and (2) prevent membrane degradation materials from clogging and occluding the stent lumen^[11]. Third, we added a PLCL outer layer without drugs to prevent an initial burst^[29]. According to the drug release curve, we successfully obtained a stable, continuous, and long-term release of GEM/CIS without an apparent initial burst, which was essential to sustain pharmacological effects without severe toxicity.

The results of the *in vitro* cell experiments and *in vivo* tumor xenograft model confirmed the antitumor activity of the drug-loaded nanofilms, and the dual-drug-loaded films showed a much better effect than the single-drug-loaded films. Interestingly, the antitumor effect of the single-drug-loaded nanofilms seemed to differ *in vitro* and *in vivo*: the PLCL-GEM nanofilm showed a stronger tumor suppression effect in the cell experiment, while the PLCL-CIS nanofilm inhibited tumor growth more potently in the tumor xenograft model. Possible reasons for these observations might be the differences in experimental parameters and drug release properties *in vitro* and *in vivo*. We used drug-released media to evaluate antitumor activity *in vitro*, and the effective drug concentration of gemcitabine was higher than that of cisplatin in the early observation period due to differences in solubility. Moreover, the incubation of drug-released media with EGI-1 cells was evaluated as a short-term effect. However, in the *in vivo* nude mouse tumor xenograft experiment, drug release was realized through direct contact together with diffusion to tumor tissue rather than simple dissolution, and the change in tumor xenografts reflected the long-term cumulative effect. Thus, the synergistic effect of dual drug loading was clarified theoretically and practically: the initial release of GEM played a dominant role in the early stage, and the compensatory release of CIS subsequently ensured the maintenance of the long-term antitumor effect.

Serological analysis *in vivo* showed that the WBC count, ALT, AST, γ -GT, and amylase levels were elevated to varying degrees: The WBC count and amylase level were only mildly increased, while the ALT, AST, and γ -GT levels were increased

moderately (3-5 × upper limit of normal). These changes were associated with transient hepatic damage secondary to the surgical procedure and gradually returned to baseline during the follow-up period in all animals^[29]. No significant differences were observed between the different stent type groups, which indicated that the serological change was not drug related or dose-dependent but rather procedure related.

Previous studies have examined the histologic influence of FCSEMS^[40] and chemotherapeutic drug-eluting stent^[6,9,11,29] placement in the bile duct, and these stents have been reported to cause an inflammatory reaction^[29,40], mucosal hyperplasia^[9], and fibrosis^[11]. In our study, no significant differences in inflammation, fibrosis, or collagenous reactions were observed between the different stent type groups. Superficial mucosal erosion with a denuded cuboidal epithelium is common for epithelial injury after stent removal^[40]. Bakhru *et al.*^[40] reported that 80% of the porcine biliary tract developed superficial mucosal erosion after the removal of temporarily placed FCSEMS^[40], and we observed a similar change in our stented groups. Moreover, epithelial layer thickness secondary to reactive hyperplasia was common and reasonable. However, no significant complications, such as lumen stenosis, occlusion, ulceration, necrosis, or perforation, were observed in any of the animals during stent implantation. Taken together, these findings of laboratory parameters and histological changes indicate that the implantation of this PLCL-GEM and CIS DES in a normal porcine bile duct is acceptable in terms of safety and feasibility.

However, our study still has several limitations. First, we tested the drug release property only *in vitro*; therefore, relevant *in vivo* data are lacking. Further studies should include drug distribution in the plasma and major organs after stent implantation. Second, we established only mouse xenograft models to study the antitumor activity of this newly designed stent *in vivo*; the results might not be representative of the real effect *in vivo* since subcutaneous tumor xenografts cannot accurately model the polymicrobial and complicated tumor microenvironment of the biliary tract. However, the corresponding large animal model of ECC in the porcine or canine biliary tract is still not available. Third, the small sample size decreased the statistical power of our results, and our study lasted for only 4 wk, which might not be sufficient for evaluation of the long-term effects after stent insertion. Thus, a larger sample size and longer observation period are needed to further assess safety and feasibility *in vivo* and to obtain reliable preclinical outcomes. Finally, we used the suture strategy, which does not correspond to clinical practice, to decrease the rates of migration after stent insertion. More reasonable modifications can be applied for anti-migration, including a modified configuration with anchoring fins, flared ends, an anchoring flap, or a larger diameter^[41].

In conclusion, we designed a novel biliary stent coated with antitumor agents (GEM and CIS), and we preliminarily confirmed its sustained local drug release and potent antitumor activity *in vitro* and *in vivo*. We anticipate that this new DES can be an alternative strategy as a fundamental component of palliative management for ECC patients and may help improve their survival and quality of life.

ARTICLE HIGHLIGHTS

Research background

Currently, extrahepatic cholangiocarcinoma (ECC) is rarely curable and associated with a poor prognosis. Effective endoscopic management is fundamental for ECC at an unresectable stage; however, the current biliary stents used clinically have shown no antitumor effect and are associated with high failure rates due to reocclusion after stent implantation.

Research motivation

DES is a new therapeutic concept for the management of ECC and may realize a combination of local chemotherapy and biliary drainage to prolong stent patency and improve prognosis. However, there have been only limited studies thus far, and all of them were only single-drug-loaded stents with a simple design and unsatisfactory efficacy. Our study was motivated by the need to develop a novel DES that can improve palliative endoscopic management for ECC. In addition, we have accumulated rich experience with sodium cholate and disodium ethylene diamine tetraacetic acid-eluting stents for the dissolution of bile duct stones in our previous studies, which aided in our current study.

Research objectives

Our study aimed to develop a novel DES coated with gemcitabine (GEM) and cisplatin (CIS)-loaded PLCL nanofilms that can maintain the continuous and long-term release of antitumor agents in the bile duct locally to inhibit tumor growth and reduce systemic toxicity.

Research methods

In our study, four different DESs were manufactured by the mixed electrospinning method, namely, bare-loaded, single-drug-loaded (GEM or CIS), and dual-drug-loaded (GEM and CIS) stents, with four drug-loading ratios (5%, 10%, 15%, and 20%). The drug release property, antitumor activity in the ECC cell line and mouse xenograft model, and biocompatibility in the normal porcine bile duct were evaluated to confirm the feasibility and efficacy of this novel DES for ECC.

Research results

We identified 10% as the appropriate drug-loading ratio based on the drug release property and inhibition efficiency. Further investigation indicated that these drug-loaded nanofilms exert ideal antitumor activity and good biosecurity.

Research conclusion

This novel PLCL-GEM and CIS-eluting stent maintains continuous, stable drug release locally and exerts potent antitumor activity *in vitro* and *in vivo*. Therefore, it might be considered an alternative strategy for the palliative therapy of ECC patients.

Research perspectives

Future studies comparing DESs and conventional systemic chemotherapy may provide more reliable evidence for the preclinical evaluation of this novel stent for the management of ECC. With development and progress in multidisciplinary therapy for cancer, it is also worth investigating the benefit of replacing systemic chemotherapy with DESs together with targeted therapy and immunotherapy in the future.

REFERENCES

- 1 **Suarez-Munoz MA**, Fernandez-Aguilar JL, Sanchez-Perez B, Perez-Daga JA, Garcia-Albiach B, Pulido-Roa Y, Marin-Camero N, Santoyo-Santoyo J. Risk factors and classifications of hilar cholangiocarcinoma. *World J Gastrointest Oncol* 2013; **5**: 132-138 [PMID: 23919107 DOI: 10.4251/wjgo.v5.i7.132]
- 2 **Esnaola NF**, Meyer JE, Karachristos A, Maranki JL, Camp ER, Denlinger CS. Evaluation and management of intrahepatic and extrahepatic cholangiocarcinoma. *Cancer* 2016; **122**: 1349-1369 [PMID: 26799932 DOI: 10.1002/cncr.29692]
- 3 **Jarnagin WR**, Fong Y, DeMatteo RP, Gonen M, Burke EC, Bodniewicz BS J, Youssef BA M, Klimstra D, Blumgart LH. Staging, resectability, and outcome in 225 patients with hilar cholangiocarcinoma. *Ann Surg* 2001; **234**: 507-17; discussion 517-9 [PMID: 11573044 DOI: 10.1097/0000658-200110000-00010]
- 4 **Abu-Hamda EM**, Baron TH. Endoscopic management of cholangiocarcinoma. *Semin Liver Dis* 2004; **24**: 165-175 [PMID: 15192789 DOI: 10.1055/s-2004-828893]
- 5 **Kim JH**. Endoscopic stent placement in the palliation of malignant biliary obstruction. *Clin Endosc* 2011; **44**: 76-86 [PMID: 22741117 DOI: 10.5946/ce.2011.44.2.76]
- 6 **Lee DK**, Kim HS, Kim KS, Lee WJ, Kim HK, Won YH, Byun YR, Kim MY, Baik SK, Kwon SO. The effect on porcine bile duct of a metallic stent covered with a paclitaxel-incorporated membrane. *Gastrointest Endosc* 2005; **61**: 296-301 [PMID: 15729251 DOI: 10.1016/s0016-5107(04)02570-2]
- 7 **Shatzel J**, Kim J, Sampath K, Syed S, Saad J, Hussain ZH, Mody K, Pipas JM, Gordon S, Gardner T, Rothstein RI. Drug eluting biliary stents to decrease stent failure rates: A review of the literature. *World J Gastrointest Endosc* 2016; **8**: 77-85 [PMID: 26839648 DOI: 10.4253/wjge.v8.i2.77]
- 8 **Lee DK**. Drug-eluting stent in malignant biliary obstruction. *J Hepatobiliary Pancreat Surg* 2009; **16**: 628-632 [PMID: 19554255 DOI: 10.1007/s00534-009-0135-1]
- 9 **Lee SS**, Shin JH, Han JM, Cho CH, Kim MH, Lee SK, Kim JH, Kim KR, Shin KM, Won YH, Song HY. Histologic influence of paclitaxel-eluting covered metallic stents in a canine biliary model. *Gastrointest Endosc* 2009; **69**: 1140-1147 [PMID: 19243763 DOI: 10.1016/j.gie.2008.08.005]
- 10 **Song TJ**, Lee SS, Yun SC, Park DH, Seo DW, Lee SK, Kim MH. Paclitaxel-eluting covered metal stents versus covered metal stents for distal malignant biliary obstruction: a prospective comparative pilot study. *Gastrointest Endosc* 2011; **73**: 727-733 [PMID: 21288514 DOI: 10.1016/j.gie.2010.11.048]
- 11 **Jang SI**, Kim JH, Kim M, Yang S, Jo EA, Lee JW, Na K, Kim JM, Jeong S, Lee DH, Lee DK. Porcine feasibility and safety study of a new paclitaxel-eluting biliary stent with a Pluronic-containing membrane. *Endoscopy* 2012; **44**: 825-831 [PMID: 22752887 DOI: 10.1055/s-0032-1309881]
- 12 **Jang SI**, Kim JH, You JW, Rhee K, Lee SJ, Kim HG, Han J, Shin IH, Park SH, Lee DK. Efficacy of a metallic stent covered with a paclitaxel-incorporated membrane versus a covered metal stent for malignant biliary obstruction: a prospective comparative study. *Dig Dis Sci* 2013; **58**: 865-871 [PMID: 23179148 DOI: 10.1007/s10620-012-2472-1]

- 13 **Shah T.** Drug-eluting stents in malignant biliary obstruction: where do we stand? *Dig Dis Sci* 2013; **58**: 610-612 [PMID: 23250674 DOI: 10.1007/s10620-012-2507-7]
- 14 **Lee JW, Yang SG, Na K.** Gemcitabine-releasing polymeric films for covered self-expandable metallic stent in treatment of gastrointestinal cancer. *Int J Pharm* 2012; **427**: 276-283 [PMID: 22366483 DOI: 10.1016/j.ijpharm.2012.02.016]
- 15 **Kim DH, Jeong YI, Chung CW, Kim CH, Kwak TW, Lee HM, Kang DH.** Preclinical evaluation of sorafenib-eluting stent for suppression of human cholangiocarcinoma cells. *Int J Nanomedicine* 2013; **8**: 1697-1711 [PMID: 23658488 DOI: 10.2147/IJN.S43508]
- 16 **Kwak TW, Lee HL, Song YH, Kim C, Kim J, Seo SJ, Jeong YI, Kang DH.** Vorinostat-eluting poly(DL-lactide-co-glycolide) nanofiber-coated stent for inhibition of cholangiocarcinoma cells. *Int J Nanomedicine* 2017; **12**: 7669-7680 [PMID: 29089762 DOI: 10.2147/IJN.S141920]
- 17 **Valle JW, Wasan H, Johnson P, Jones E, Dixon L, Swindell R, Baka S, Maraveyas A, Corrie P, Falk S, Gollins S, Lofts F, Evans L, Meyer T, Anthony A, Iveson T, Highley M, Osborne R, Bridgewater J.** Gemcitabine alone or in combination with cisplatin in patients with advanced or metastatic cholangiocarcinomas or other biliary tract tumours: a multicentre randomised phase II study - The UK ABC-01 Study. *Br J Cancer* 2009; **101**: 621-627 [PMID: 19672264 DOI: 10.1038/sj.bjc.6605211]
- 18 **Valle J, Wasan H, Palmer DH, Cunningham D, Anthony A, Maraveyas A, Madhusudan S, Iveson T, Hughes S, Pereira SP, Roughton M, Bridgewater J; ABC-02 Trial Investigators.** Cisplatin plus gemcitabine versus gemcitabine for biliary tract cancer. *N Engl J Med* 2010; **362**: 1273-1281 [PMID: 20375404 DOI: 10.1056/NEJMoa0908721]
- 19 **Miyazaki M, Yoshitomi H, Miyakawa S, Uesaka K, Unno M, Endo I, Ota T, Ohtsuka M, Kinoshita H, Shimada K, Shimizu H, Tabata M, Chijiwa K, Nagino M, Hirano S, Wakai T, Wada K, Isayama H, Okusaka T, Tsuyuguchi T, Fujita N, Furuse J, Yamao K, Murakami K, Yamazaki H, Kijima H, Nakanuma Y, Yoshida M, Takayashiki T, Takada T.** Clinical practice guidelines for the management of biliary tract cancers 2015: the 2nd English edition. *J Hepatobiliary Pancreat Sci* 2015; **22**: 249-273 [PMID: 25787274 DOI: 10.1002/jhbp.233]
- 20 **Okusaka T, Nakachi K, Fukutomi A, Mizuno N, Ohkawa S, Funakoshi A, Nagino M, Kondo S, Nagaoka S, Funai J, Koshiji M, Nambu Y, Furuse J, Miyazaki M, Nimura Y.** Gemcitabine alone or in combination with cisplatin in patients with biliary tract cancer: a comparative multicentre study in Japan. *Br J Cancer* 2010; **103**: 469-474 [PMID: 20628385 DOI: 10.1038/sj.bjc.6605779]
- 21 **Sun TT, Wang JL, Fang JY.** Gemcitabine alone or in combination with Cisplatin for advanced biliary tract carcinomas: an overview of clinical evidence. *Asian Pac J Cancer Prev* 2013; **14**: 877-883 [PMID: 23621255 DOI: 10.7314/apjcp.2013.14.2.877]
- 22 **Razumilava N, Gores GJ.** Cholangiocarcinoma. *Lancet* 2014; **383**: 2168-2179 [PMID: 24581682 DOI: 10.1016/S0140-6736(13)61903-0]
- 23 **Benson AB, D'Angelica MI, Abbott DE, Abrams TA, Alberts SR, Anaya DA, Anders R, Are C, Brown D, Chang DT, Cloyd J, Covey AM, Hawkins W, Iyer R, Jacob R, Karachristos A, Kelley RK, Kim R, Palta M, Park JO, Sahai V, Scheffter T, Sicklick JK, Singh G, Sohal D, Stein S, Tian GG, Vauthey JN, Venook AP, Hammond LJ, Darlow SD.** Guidelines Insights: Hepatobiliary Cancers, Version 2.2019. *J Natl Compr Canc Netw* 2019; **17**: 302-310 [PMID: 30959462 DOI: 10.6004/jnccn.2019.0019]
- 24 **Liu J, Wang Z, Wu K, Li J, Chen W, Shen Y, Guo S.** Paclitaxel or 5-fluorouracil/esophageal stent combinations as a novel approach for the treatment of esophageal cancer. *Biomaterials* 2015; **53**: 592-599 [PMID: 25890755 DOI: 10.1016/j.biomaterials.2015.03.009]
- 25 **Wang Z, Liu J, Wu K, Shen Y, Mao A, Li J, Chen Z, Guo S.** Nitinol stents loaded with a high dose of antitumor 5-fluorouracil or paclitaxel: esophageal tissue responses in a porcine model. *Gastrointest Endosc* 2015; **82**: 153-160.e1 [PMID: 25936448 DOI: 10.1016/j.gie.2015.02.034]
- 26 **Moon S, Yang SG, Na K.** An acetylated polysaccharide-PTFE membrane-covered stent for the delivery of gemcitabine for treatment of gastrointestinal cancer and related stenosis. *Biomaterials* 2011; **32**: 3603-3610 [PMID: 21334742 DOI: 10.1016/j.biomaterials.2011.01.070]
- 27 **Li G, Chen Y, Hu J, Wu X, Hu J, He X, Li J, Zhao Z, Chen Z, Li Y, Hu H, Li Y, Lan P.** A 5-fluorouracil-loaded polydioxanone weft-knitted stent for the treatment of colorectal cancer. *Biomaterials* 2013; **34**: 9451-9461 [PMID: 24011711 DOI: 10.1016/j.biomaterials.2013.08.055]
- 28 **Suk KT, Kim JW, Kim HS, Baik SK, Oh SJ, Lee SJ, Kim HG, Lee DH, Won YH, Lee DK.** Human application of a metallic stent covered with a paclitaxel-incorporated membrane for malignant biliary obstruction: multicenter pilot study. *Gastrointest Endosc* 2007; **66**: 798-803 [PMID: 17905025 DOI: 10.1016/j.gie.2007.05.037]
- 29 **Chung MJ, Kim H, Kim KS, Park S, Chung JB, Park SW.** Safety evaluation of self-expanding metallic biliary stents eluting gemcitabine in a porcine model. *J Gastroenterol Hepatol* 2012; **27**: 261-267 [PMID: 21793905 DOI: 10.1111/j.1440-1746.2011.06866.x]
- 30 **Kwak TW, Kim DH, Jeong YI, Kang DH.** Antitumor activity of vorinostat-incorporated nanoparticles against human cholangiocarcinoma cells. *J Nanobiotechnology* 2015; **13**: 60 [PMID: 26410576 DOI: 10.1186/s12951-015-0122-4]
- 31 **Tringali A, Mutignani M, Adler DG.** Fully covered self-expandable metal stents versus uncovered self-expandable metal stents in patients with distal malignant biliary stricture: Is this the right question? *Gastrointest Endosc* 2019; **89**: 897-898 [PMID: 30902212 DOI: 10.1016/j.gie.2018.09.031]
- 32 **Jang S, Stevens T, Parsi M, Lopez R, Zuccaro G, Dumot J, Vargo JJ.** Association of covered metallic stents with cholecystitis and stent migration in malignant biliary stricture. *Gastrointest Endosc* 2018; **87**: 1061-1070 [PMID: 28867074 DOI: 10.1016/j.gie.2017.08.024]
- 33 **Conio M, Mangiavillano B, Caruso A, Filiberti RA, Baron TH, De Luca L, Signorelli S, Crespi M, Marini M, Ravelli P, Conigliaro R, De Ceglie A.** Covered versus uncovered self-expandable metal stent for palliation of primary malignant extrahepatic biliary strictures: a randomized multicenter study. *Gastrointest Endosc* 2018; **88**: 283-291.e3 [PMID: 29653120 DOI: 10.1016/j.gie.2018.03.029]
- 34 **Isayama H, Komatsu Y, Tsujino T, Sasahira N, Hirano K, Toda N, Nakai Y, Yamamoto N, Tada M, Yoshida H, Shiratori Y, Kawabe T, Omata M.** A prospective randomised study of "covered" versus "uncovered" diamond stents for the management of distal malignant biliary obstruction. *Gut* 2004; **53**: 729-

- 734 [PMID: 15082593 DOI: 10.1136/gut.2003.018945]
- 35 **Isayama H**, Kawabe T, Nakai Y, Ito Y, Togawa O, Kogure H, Yashima Y, Yagioka H, Matsubara S, Sasaki T, Sasahira N, Hirano K, Tsujino T, Tada M, Omata M. Management of distal malignant biliary obstruction with the ComVi stent, a new covered metallic stent. *Surg Endosc* 2010; **24**: 131-137 [PMID: 19517184 DOI: 10.1007/s00464-009-0537-9]
- 36 **Tringali A**, Hassan C, Rota M, Rossi M, Mutignani M, Aabakken L. Covered vs. uncovered self-expandable metal stents for malignant distal biliary strictures: a systematic review and meta-analysis. *Endoscopy* 2018; **50**: 631-641 [PMID: 29342491 DOI: 10.1055/s-0043-125062]
- 37 **Silvis SE**, Sievert CE Jr, Vennes JA, Abeyta BK, Brennecke LH. Comparison of covered versus uncovered wire mesh stents in the canine biliary tract. *Gastrointest Endosc* 1994; **40**: 17-21 [PMID: 8163131 DOI: 10.1016/s0016-5107(94)70004-4]
- 38 **Kim JY**, Ko GB, Lee TH, Park SH, Lee YN, Cho YS, Jung Y, Chung IK, Choi HJ, Cha SW, Moon JH, Cho YD, Kim SJ. Partially Covered Metal Stents May Not Prolong Stent Patency Compared to Uncovered Stents in Unresectable Malignant Distal Biliary Obstruction. *Gut Liver* 2017; **11**: 440-446 [PMID: 28208003 DOI: 10.5009/gnl16245]
- 39 **Beyna T**, Neuhaus H. Self-expandable metal stents in malignant biliary obstruction: Back to the roots with uncovered stents as the "new" standard? *Gastrointest Endosc* 2018; **87**: 1071-1073 [PMID: 29571772 DOI: 10.1016/j.gie.2017.11.022]
- 40 **Bakhru MR**, Foley PL, Gatesman J, Schmitt T, Moskaluk CA, Kahaleh M. Fully covered self-expanding metal stents placed temporarily in the bile duct: safety profile and histologic classification in a porcine model. *BMC Gastroenterol* 2011; **11**: 76 [PMID: 21689439 DOI: 10.1186/1471-230X-11-76]
- 41 **Lee HW**, Moon JH, Lee YN, Lee TH, Choi MH, Cha SW, Cho YD, Park SH. Usefulness of newly modified fully covered metallic stent of 12 mm in diameter and anti-migration feature for periampullary malignant biliary strictures: Comparison with conventional standard metal stent. *J Gastroenterol Hepatol* 2019; **34**: 1208-1213 [PMID: 30650205 DOI: 10.1111/jgh.14602]



Published by **Baishideng Publishing Group Inc**
7041 Koll Center Parkway, Suite 160, Pleasanton, CA 94566, USA
Telephone: +1-925-3991568
E-mail: bpgoffice@wjgnet.com
Help Desk: <https://www.f6publishing.com/helpdesk>
<https://www.wjgnet.com>

